

Slow Conformational Dynamics and Unfolding of the Calmodulin C-Terminal Domain

Yng-Gwei Chen and Gerhard Hummer*

Laboratory of Chemical Physics, Building 5, National Institute of Diabetes and Digestive and Kidney Diseases, National Institutes of Health, Bethesda, Maryland 20892-0520

Received October 31, 2006; E-mail: gerhard.hummer@nih.gov

Calmodulin (CaM) is a calcium-sensing protein whose physiological function requires large-scale conformational changes. CaM is ubiquitous among eukaryotes with a highly conserved sequence. Two globular domains are connected by a flexible central linker.¹ Each domain presents two Ca²⁺ binding sites in an EF-hand helix–loop–helix motif.^{2,3} Upon Ca²⁺ binding, the structures of the CaM domains change from a relatively compact, “closed” apo conformation to a more “open” holo conformation that partially exposes the hydrophobic interior of the protein.^{4–10} The open holo conformations enable subsequent binding to a wide range of targets that are involved in numerous cellular processes, such as gene regulation, cytoskeletal organization, muscle contraction, signal transduction, ion homeostasis, exocytosis, and metabolic regulation.¹¹

The plasticity of CaM is thought to be essential for binding to its many different protein targets. Significant interdomain as well as intradomain motions have been implied from differences between crystal and solution structures^{1,12–15} and observed in dynamics measurements.^{16–18} Even in the absence of Ca²⁺, NMR studies of the isolated C-terminal domain identified large structural changes on the μ s to ms time scale that leave the secondary structure largely intact.^{16,17} However, the original interpretation of the observed slow dynamics in terms of transitions between apo and holo-like forms has recently been challenged based on T-jump fluorescence experiments.¹⁹ Those experiments suggested that the C-terminal domain simply undergoes a two-state folded to unfolded transition. Indeed, in the absence of Ca²⁺, the melting temperature T_f of the isolated C-terminal domain is remarkably low (323 K), and it is even lower in the intact CaM (\sim 315 K), close to physiological temperatures (37 °C; 310 K).²⁰ Rabl et al.¹⁹ employed a two-state model for the unfolding of the domain, and their measured and fitted relaxation times at the temperature of the NMR experiments (\sim 20 °C) were found to be about 200 μ s, close to the exchange times (35–350 μ s) of the slow transitions found in NMR experiments.^{16,17}

To investigate these conflicting interpretations, we carry out simulations of the wild-type CaM C-terminal domain using a coarse-grained Hamiltonian. In addition to the protein structures, the model is constructed to satisfy the experimental melting temperature T_f , the relative populations of the open and closed conformations at 18 °C, and the exchange rate between them.^{17,22} From our simulations emerges a three-state picture that reconciles the seemingly contradictory experimental findings: the three states include a folded state with apo structures (closed), an unfolded state, and a “holo-like” state (open) which is rather floppy without bound Ca²⁺ and structurally less defined.

Structure-based coarse models for proteins, such as elastic network and G \bar{o} models, have had considerable success in studies of protein folding and dynamics.²¹ In these models, the experimental structure is built in as the *only* major minimum of the free energy under native conditions. However, the CaM domains each assume

different major apo and holo conformations, with the C-terminal domain likely to have noticeable holo-like conformers in the absence of Ca²⁺. Several generalizations have recently been proposed to construct coarse Hamiltonians that accommodate multiple folded conformations.^{22,23} Here, we construct a hybrid coarse Hamiltonian H using a C_α representation with pseudodihedral angles and 12–10 attractive residue interactions.²² H is defined through $\exp(-\beta'H) = \exp(-\beta'H_{\text{apo}}) + \exp[-\beta'(H_{\text{holo}} + \epsilon)]$. H_{apo} and H_{holo} are residue-level coarse Hamiltonians built from the Ca²⁺-free and the Ca²⁺-ligated forms of the domain, respectively. ϵ controls the relative stability of the H_{apo} and H_{holo} basins, while the mixing parameter β' determines the barrier height between the H_{apo} and H_{holo} energy minima. ϵ and $(\beta')^{-1}$ are set to 5.33 and 2 kcal/mol, respectively.

Long equilibrium simulations were carried out at temperatures ranging from 270 to 350 K. To correct for the low damping coefficient used (0.1 ps⁻¹, \sim 1/1000 of that typical of water), time is scaled by 1000. For a similar model, such scaling was shown to be accurate to within about a factor of 3.²⁶ The Langevin dynamics trajectories were analyzed jointly to compute the heat capacity $C(T)$ (Figure 1a). The $C(T)$ curve peaks at about 325 K, which is close to the T_f (49.4 °C) of an isolated fragment of the C-terminal domain. By construction, the model recovers the relative population of open conformations ($<$ 10%) and the exchange rate k_{ex} (28000 s⁻¹; 18 °C) of the closed/open transitions estimated from NMR experiments by Malmendal et al.¹⁷ In addition, the folding/unfolding relaxation rates are predicted within about a factor of 10 of those measured for full-length CaM¹⁹ (Figure 1b).

To quantify structural changes, we use (1) the root-mean-square distance (rmsd_{apo}) to the apo form and (2) the difference $Q_{\text{diff}} = Q_{\text{apo}} - Q_{\text{holo}}$ in the fraction of native amino acid contacts.²² Positive and negative Q_{diff} values indicate apo and holo-like states, respectively. The Q_{diff} and rmsd trajectories in Figure 2 capture transitions between those two states.

2-Dimensional probability maps (Figure 3) show that the high-rmsd excursions from the apo state seen in Figure 2 (bottom) give rise to a third basin corresponding to (partially) unfolded structures, in addition to the apo (closed, well folded) and holo-like states (open and less ordered). At 300 K, the populations of the three states are about 90% (apo/folded), 1% (apo/unfolded), and 9% (holo-like). The unfolded state becomes more populated than the holo-like state above \sim 314 K, where the folded apo state still dominates.

To relate our simulations to the T-jump fluorescence spectroscopy experiments, we define N_{Y138} as the number of residues within 8 Å of the fluorescence probe Tyr138. As shown in Figure 1b, the temperature-dependent relaxation rate $1/\tau$ calculated from the autocorrelation function of N_{Y138} exhibits the S-shape of the experimental data,¹⁹ with an inflection point near T_f . Above \sim 320 K, the relaxation is dominated by unfolding transitions, consistent with the interpretation of Rabl et al.¹⁹ In contrast, below \sim 300 K

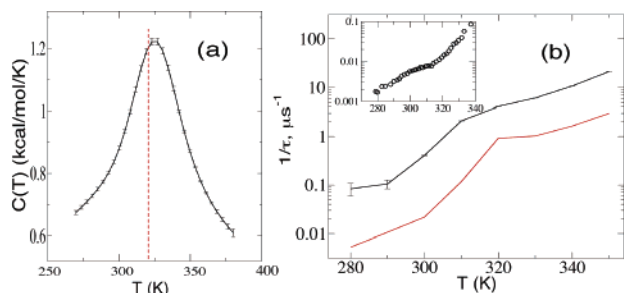


Figure 1. Thermodynamics and kinetics of CaM conformational transitions. (a) Calculated heat capacity of the CaM C-terminal domain. The red dashed line indicates the experimentally measured melting temperature, $T_f \approx 322.4$ K.²⁰ (b) Tyr138 relaxation dynamics estimated from fluctuations in N_{Y138} , the number of residues within 8 Å of Tyr138 (integrated correlation time, black line; exponential decay at long times, red line). The inset shows the inverse characteristic times measured in T-jump tyrosine absorption experiments.¹⁹ Note that full-length CaM was used in those experiments, accounting for the slight shift in temperature²⁰ (~ 10 K) and time scales (~ 10).

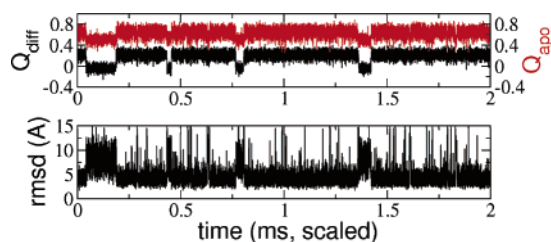


Figure 2. Equilibrium simulation at 300 K projected onto Q_{apo} (red, top), Q_{diff} (black, top), and $rmsd_{apo}$ (bottom).

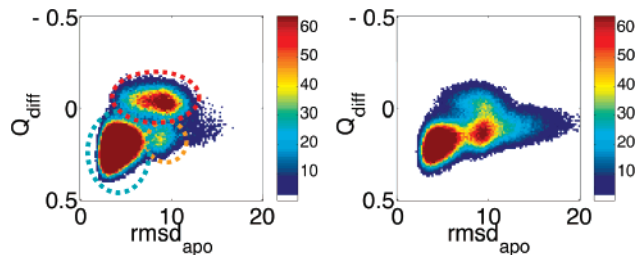


Figure 3. Joint probability distributions of Q_{diff} and $rmsd_{apo}$ (Å) at (left) 300 K and (right) 320 K. The blue, red, and orange dashed ovals indicate the apo basin, the hololike basin, and the (partially) unfolded states, respectively. Note the inverted Q_{diff} axis with apolike states at the bottom.

the exchange is predominantly between folded apo and hololike states, consistent with the interpretation of a closed/open transition inferred from NMR. At 300 K, the relaxation rate is about 22000 s^{-1} (Figure 1b), close to the targeted NMR k_{ex} value. Qualitatively, this three-state scenario could have been postulated simply from the low melting temperature and the closed/open transitions inferred from the NMR experiments. In addition, our molecular model provides not only a detailed picture of the associated conformational changes but also explains the *apparent* two-state behavior.¹⁹ We find that the crossover from low- T open/closed transitions to high- T folded/unfolded transitions occurs over a narrow temperature window, with the respective “third state” always having a low population.

Remarkably, the regime in which all three states have significant populations is around physiological temperatures (37 °C; 310 K). At these temperatures, a significant population of partially unfolded CaM is supported by folding thermodynamics data,²⁰ as well as a recent NMR experiment revealing transient partial unfolding of a

helix in the C-terminal domain.¹⁸ Such partial unfolding is also reminiscent of cold denaturation.²⁴ The more dynamic character of the C-terminal domain, compared to the N-terminal domain, is evident in lower protection factors for hydrogen exchange.¹⁶ The equilibrium of closed, open, and unfolded Ca^{2+} -free states may simply be a byproduct of the conformational plasticity required for CaM binding to a wide variety of peptide substrates; alternatively, the unfolded apo state may have direct functional relevance, for example, in target peptide binding or as an intermediate in the Ca^{2+} -induced apo-to-holo transition. Together with many other proteins,²⁵ in particular kinase targets involved in signaling, CaM challenges the paradigm that functionally important structures are dominated by a single, stably folded conformation.

Acknowledgment. We thank Drs. Ad Bax, Robert Best, and Claude Klee for many helpful and stimulating discussions. This research was supported by the Intramural Research Programs of the NIH, NIDDK.

Supporting Information Available: Details of the coarse Hamiltonian and simulations. This material is available free of charge via the Internet at <http://pubs.acs.org>.

References

- (1) Barbato, G.; Ikura, M.; Kay, L. E.; Pastor, R. W.; Bax, A. *Biochemistry* **1992**, *31*, 5269–5278.
- (2) (a) Kretsinger, R. H.; Nockolds, C. E. *J. Biol. Chem.* **1973**, *248*, 3313–3326. (b) Kretsinger, R. H. *Cold Spring Harbor Symp. Quant. Biol.* **1987**, *52*, 499–510.
- (3) Linse, S.; Helmersson, A.; Forsén, S. *J. Biol. Chem.* **1991**, *266*, 8050–8054.
- (4) Kuboniwa, H.; Tjandra, N.; Grzesiek, S.; Ren, H.; Klee, C. B.; Bax, A. *Nat. Struct. Biol.* **1995**, *2*, 768–776.
- (5) Zhang, M.; Tanaka, T.; Ikura, M. *Nat. Struct. Biol.* **1995**, *2*, 758–767.
- (6) Babu, Y. S.; Bugg, C. E.; Cook, W. J. *J. Mol. Biol.* **1988**, *204*, 191–204.
- (7) Chattopadhyaya, R.; Meador, W. E.; Means, A. R.; Quijcho, F. A. *J. Mol. Biol.* **1992**, *228*, 1177–1192.
- (8) Nelson, M. R.; Chazin, W. J. *Protein Sci.* **1998**, *7*, 270–282.
- (9) Finn, B. E.; Evenäs, J.; Drakenberg, T.; Waltho, J. P.; Thulin, E.; Forsén, S. *Nat. Struct. Biol.* **1995**, *2*, 777–783.
- (10) Vigil, D.; Gallagher, S. C.; Trehwella, J.; García, A. E. *Biophys. J.* **2001**, *80*, 2082–2092.
- (11) *Guidebook to the Calcium-Binding Proteins*; Celio, M. R.; Pauls T.; Schwaller, B., Eds.; Oxford University Press: New York, 1996.
- (12) Heidorn, D. B.; Trehwella, J. *Biochemistry* **1988**, *27*, 909–915.
- (13) Chou, J. J.; Li, S. P.; Klee, C. B.; Bax, A. *Nat. Struct. Biol.* **2001**, *8*, 990–997.
- (14) Meador, W. E.; Means, A. R.; Quijcho, F. A. *Science* **1993**, *262*, 1718–1721.
- (15) Wilson, M. A.; Brunger, A. T. *J. Mol. Biol.* **2000**, *301*, 1237–1256.
- (16) Tjandra, N.; Kuboniwa, H.; Ren, H.; Bax, A. *Eur. J. Biochem.* **1995**, *230*, 1014–1024.
- (17) Malmendal, A.; Evenäs, J.; Forsén, S.; Akke, M. *J. Mol. Biol.* **1999**, *293*, 883–899.
- (18) Lundström, P.; Mulder, F. A. A.; Akke, M. *Proc. Natl. Acad. Sci. U.S.A.* **2005**, *102*, 16984–16989.
- (19) Rabl, C.-R.; Martin, S. R.; Neumann, E.; Bayley, P. M. *Biophys. Chem.* **2002**, *101*, 553–564.
- (20) Masino, L.; Martin, S. R.; Bayley, P. M. *Protein Sci.* **2000**, *9*, 1519–1529.
- (21) See for example: (a) Karanicolas, J.; Brooks, C. L. *Protein Sci.* **2002**, *11*, 2351–2361. (b) Chavez, L. L.; Onuchic, J. N.; Clementi, C. *J. Am. Chem. Soc.* **2004**, *126*, 8426–8432.
- (22) Best, R. B.; Chen, Y.-G.; Hummer, G. *Structure* **2005**, *13*, 1755–1763.
- (23) (a) Zuckerman, D. M. *J. Phys. Chem. B* **2004**, *108*, 5127–5137. (b) Maragakis, P.; Karplus, M. *J. Mol. Biol.* **2005**, *352*, 807–822. (c) Koga, N.; Takada, S. *Proc. Natl. Acad. Sci. U.S.A.* **2006**, *103*, 5367–5372. (d) Okazaki, K.; Koga, N.; Takada, S.; Onuchic, J. N.; Wolynes, P. G. *Proc. Natl. Acad. Sci. U.S.A.* **2006**, *103*, 11844–11849.
- (24) Whitten, S. T.; Kurtz, A. J.; Pometun, M. S.; Wand, A. J.; Hilsner, V. J. *Biochemistry* **2006**, *45*, 10163–10174.
- (25) (a) Dunker, A. K.; Brown, C. J.; Lawson, J. D.; Iakoucheva, L. M.; Obradovic, Z. *Biochemistry* **2002**, *41*, 6573–6582. (b) Iakoucheva, L. M.; Radiwojac, P.; Brown, C. J.; O’Connor, T. R.; Sikes, J. G.; Obradovic, Z.; Dunker, A. K. *Nucleic Acids Res.* **2004**, *32*, 1037–1049. (c) Tompa, P. *Trends Biochem. Sci.* **2002**, *27*, 527–533.
- (26) Best, R. B.; Hummer, G. *Phys. Rev. Lett.* **2006**, *96*, 228104.

JA067791A